Magnetic Properties

A Reductive-Aggregation Route to $[Mn_{12}O_{12}(OMe)_2(O_2CPh)_{16}(H_2O)_2]^{2-}$ Single-Molecule Magnets Related to the $[Mn_{12}]$ Family**

*Anastasios J. Tasiopoulos, Wolfgang Wernsdorfer, Khalil A. Abboud, and George Christou**

An exciting development in nanoscale magnetic materials occurred in 1993 when $[Mn_{12}O_{12}(O_2CMe)_{16}(H_2O)_4]$ (**1**) was identified as a nanoscale magnet,[1] the first to comprise discrete, (magnetically) non-interacting molecular units rather than a 3D extended lattice (as in metals and metal oxides, for example). This discovery initiated the field of

[*] Dr. A. J. Tasiopoulos,[+] Dr. K. A. Abboud, Prof. Dr. G. Christou
Department of Chemistry
University of Florida
Gainesville, FL 32611-7200 (USA)
Fax: (+1) 352-392-8757
E-mail: christou@chem.ufl.edu
Dr. W. Wernsdorfer
Laboratoire Louis Néel-CNRS
BP 166, 25 Avenue des Martyrs, 38042 Grenoble, Cedex 9 (France)
[+] present address:
Department of Chemistry
University of Cyprus, 1678 Nicosia (Cyprus)

[**] This work was supported by the National Science Foundation.

  DOI: 10.1002/ange.200461551

molecular nanomagnetism and such molecules have since been termed single-molecule magnets (SMMs).[2] They derive their properties from the combination of a large spin (S) and an Ising (easy-axis) magnetoanisotropy (negative zero-field splitting parameter, D). Although several classes of SMMs are now known,[1–10] there is still a need for new examples to improve our understanding of this phenomenon. Efforts along these lines have been concentrated in two directions: 1) development of synthetic routes to new high nuclearity metal complexes,[4,5] and 2) modifications of known SMMs in a controlled fashion.[6–10] The best and most thoroughly studied SMMs to date are members of the $[Mn_{12}O_{12}(O_2CR)_{16}(H_2O)_4]$ ($[Mn_{12}]$) family. A number of $[Mn_{12}]$ derivatives have been prepared in their neutral,[1,6–8] one-electron[6f,9] or two-electron[10] reduced versions with a variety of carboxylate,[6,9,10] mixed carboxylate,[7] and mixed carboxylate/non-carboxylate[8] ligands. In all such modifications, the $[Mn_{12}(\mu_3\text{-}O)_{12}]$ core remains essentially the same.

Herein, we report three new developments: 1) a new synthetic procedure in manganese cluster chemistry involving reductive aggregation of permanganate ($[MnO_4]^-$) ions in MeOH/benzoic acid solution; 2) its employment to synthesize NnBu$_4^+$ salts of the new $[Mn_{12}O_{12}(OMe)_2(O_2CPh)_{16}(H_2O)_2]^{2-}$ cluster ion, which is a structural derivative of the well studied $[Mn_{12}]$ complexes; and 3) the establishment that this anion is a new SMM.

The synthesis of normal $[Mn_{12}]$ compound **1** consists of the comproportionation reaction between $Mn(O_2CMe)_2{\cdot}4H_2O$ and $KMnO_4$ in 60% aqueous acetic acid.[11] In contrast, the new synthetic procedure herein is part of a wider investigation of the reduction of $[MnO_4]^-$ in alcohol/carboxylic acid mixtures. The present results were obtained from a MeOH/$PhCO_2H$ medium. Thus, addition of (NnBu$_4$)MnO_4 to a methanolic solution of benzoic acid results in the formation of a dark brown solution from which subsequently were obtained essentially black crystals. Recrystallization from CH_2Cl_2/hexanes results in the formation of two types of black crystals in a total, overall yield of 15%.

Both types of crystals, diamond-like **2a** and needle-like **2b**, were crystallographically characterized. Both contain the same dianion, abbreviated $[Mn'_{12}]^{2-}$.

$(N\mathit{n}Bu_4)_2[Mn_{12}O_{12}(OMe)_2(O_2CPh)_{16}(H_2O)_2]\cdot 2H_2O\cdot 4CH_2Cl_2$ **2a**

$(N\mathit{n}Bu_4)_2[Mn_{12}O_{12}(OMe)_2(O_2CPh)_{16}(H_2O)_2]\cdot 2H_2O\cdot CH_2Cl_2$ **2b**

Complex **2a**[12] crystallizes in the orthorhombic space group *Pbca* with its asymmetric unit containing half the $[Mn'_{12}]^{2-}$cluster and one $[N\mathit{n}Bu_4]^+$ ion, as well as one H_2O and two disordered CH_2Cl_2 solvent molecules. The $[Mn'_{12}]^{2-}$ ion of **2a** (Figure 1) contains a central $[Mn^{IV}_4(\mu_3\text{-}O)_2(\mu\text{-}O)_2(\mu\text{-}OMe)_2]^{6+}$ unit surrounded by a nonplanar ring of eight Mn^{III} atoms that are connected to the central Mn_4 unit by eight bridging μ_3-O^{2-} ions. The metal oxidation states and their trapped-valence nature were determined by inspection of the Mn–O bond lengths, manganese bond valence sum calculations,[13] and the presence of Mn^{III} Jahn–Teller elongation axes for the manganese atoms in the outer ring. The outer Mn_8 ring is very similar to that in normal $[Mn_{12}]$ compound **1**, but **1** has

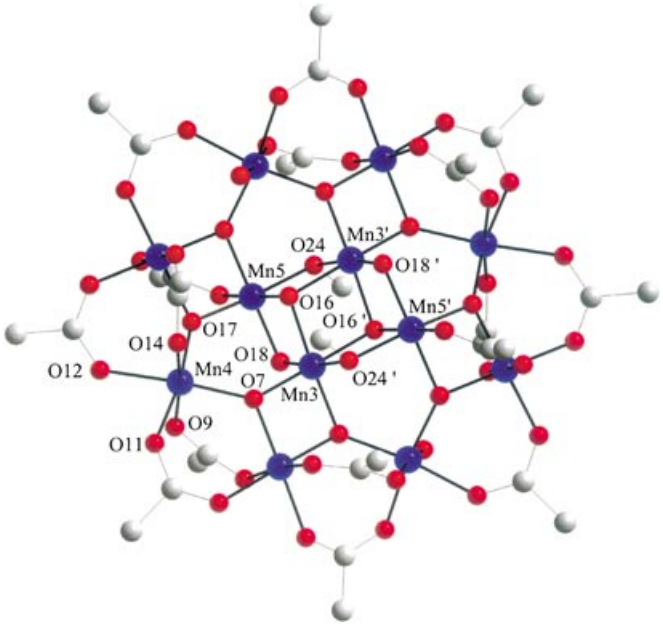

Figure 1. ORTEP plot (thermal ellipsoids set at 50% probability) of the anion of **2a**. For clarity, the benzoate rings have been omitted, except for the *ipso*-carbon atom of each ring; Mn blue, O red, C gray.

a central $[Mn_4(\mu_3\text{-}O)_4]^{8+}$ cubane. The central $[Mn^{IV}_4O_4(OMe)_2]^{6+}$ unit of **2a** comprises a planar Mn_4 rhombus with two μ_3-O^{2-} ions (O16, O16′), one above and one below the Mn_4 plane, and a μ-O^{2-} (O18, O18′) or μ-MeO^- (O24, O24′) ion bridging each edge of the rhombus. The central unit can thus be described either as a face-sharing dicubane unit with two missing vertices, or as two edge-sharing, oxide-capped Mn_3 triangular units; tetranuclear complexes possessing a core very similar to this central unit have been observed with manganese,[5a,b] as well as with other transition metals.[14] Peripheral ligation is completed by 16 bridging benzoate groups and two terminal water molecules. All the manganese atoms are six-coordinate with near octahedral coordination geometries.

Complex **2b** crystallizes in the triclinic space group $P\bar{1}$,[12a] and its asymmetric unit consists of a half cluster and two halves of $[N\mathit{n}Bu_4]^+$ ions disordered around inversion centers, as well as one disordered H_2O molecule and half a CH_2Cl_2. The structure of the anion of **2b** is essentially identical to that of **2a**, except for some disorder in the peripheral benzoate rings.

For both **2a** and **2b**, there are Jahn–Teller (JT) distortions at the Mn^{III} ions in the outer ring, consistent with high-spin Mn^{III} centers with near-octahedral coordination geometry. The JT distortion takes the form of an axial elongation, with the elongation axes axial to the Mn_{12} disk-like core and thus roughly parallel to each other. Axially elongated Mn–O bonds are typically at least 0.1–0.2 Å longer than the others. However, there is one anomaly: for **2a** (Figure 1), the JT elongated bonds at Mn4 (Mn4–O9 2.074(4), Mn4–O14 2.080(5) Å) are not as long as those found at the other Mn^{III} ions (2.112(5)–2.250(5) Å), and the *trans* bonds Mn4–O7 (1.958(4) Å) and Mn4–O12 (2.060(5) Å) are longer than expected, especially Mn4–O7, which is unusually long for an

Mn-O^{2-} bond (compare Mn–O^{2-} bonds at the other Mn^{III} ions of 1.876(4)–1.905(4) Å). A similar anomalous situation is present at Mn1 of **2b**. This structural feature at manganese atoms Mn4 of **2a** and Mn1 of **2b** is crucial to understanding the magnetic data (see below).

The anions of complexes **2a** and **2b** are remarkably similar to normal $[Mn_{12}]$ clusters, such as **1**, with the main difference being the structure of the central cores (Figure 2).

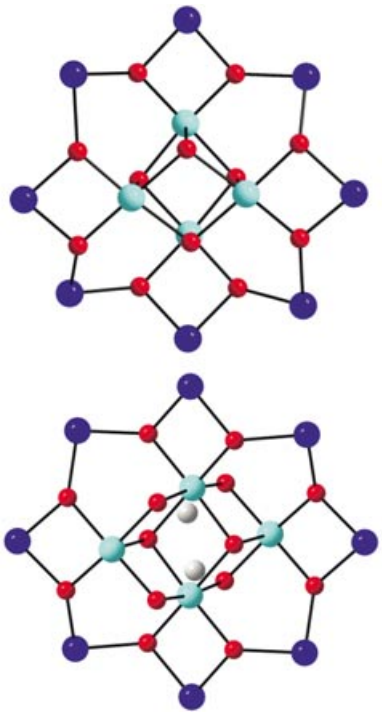

Figure 2. Comparison of the cores of normal $[Mn_{12}]$ complex **1** (top) and the anion of **2a** (bottom); Mn^{4+} cyan, Mn^{3+} blue, O red, C gray.

The core of the anions of **2a** and **2b** could be considered the result of partial methanolysis of the central $[Mn_4O_4]^{8+}$ cubane of **1**, leading to incorporation of two MeO^- bridges and a change in the core structure (although we do not claim that this corresponds to its means of formation in the reaction mixture). Note that complexes **1** and **2** are the smallest nuclearity members of a larger family of $[Mn^{III}_x,Mn^{IV}_y]$ clusters in which there is an outer Mn^{III}_x ring around a central Mn^{IV}_y core. This family currently comprises normal $[Mn_{12}]$ complexes (such as **1**) and **2a**/**2b** ($x=8$, $y=4$), the Mn_{16} cluster $[Mn_{16}O_{16}(OMe)_6(O_2CMe)_{16}(MeOH)_3(H_2O)_3]$ ($x=10$, $y=6$),[4c,15] and the Mn_{21} cluster $[Mn_{21}O_{24}(OMe)_8(O_2CCH_2$-$tBu)_{16}(H_2O)_{10}]$ ($x=12$, $y=9$).[16]

The structural similarity between complexes **1** and **2** suggested that **2** might also be an SMM. Thus AC magnetic susceptibility measurements were performed on a polycrystalline sample of **2** (containing both **2a** and **2b**) in the temperature range 1.8–10 K using a 3.5 G AC field oscillating at 5–500 Hz frequencies (ν). These studies revealed two frequency-dependent out-of-phase (χ_m'') AC signals (Figure 3), one in the higher temperature (HT) range of 3–5 K, and a second one at lower temperatures (LT) whose

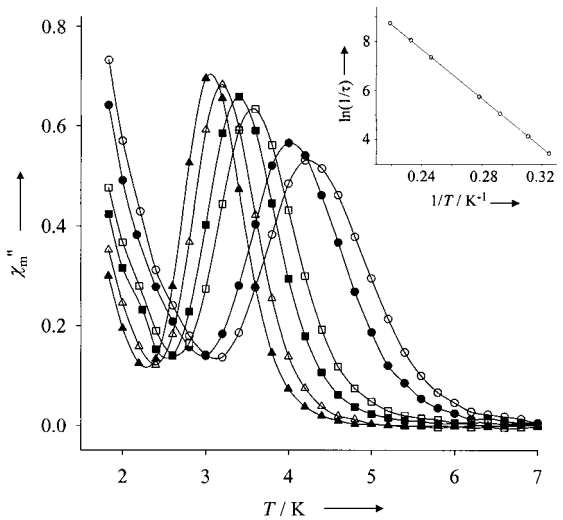

Figure 3. Plot of χ_m'' versus T for a microcrystalline sample of **2** suspended in solid eicosane at 500 (○), 250 (●), 50 (□), 25 (■), 10 (△), 5 Hz (▲). Inset: Plot of the natural logarithm of relaxation rate, ln(1/τ) versus inverse temperature using the χ_m'' versus T data for the slower relaxing species (higher temperature data). The solid line is a fit to the Arrhenius equation; see the text for the fitting parameters.

peaks clearly occur at temperatures below the operating limit of our SQUID (superconducting quantum interference device) instrument (1.8 K). The LT and HT χ_m'' signals correspond to faster and slower relaxation rates, respectively. The peak of a χ_m'' versus T plot represents the temperature at which the magnetization relaxation rate equals the angular frequency $\omega(=2\pi\nu)$, and the χ_m'' versus T data at different frequencies (ν) were therefore used as a source of kinetic data to construct an Arrhenius plot (Figure 3, inset) based on the Arrhenius equation in Equation (1), where $1/\tau$ is the relax-

$$1/\tau = 1/\tau_0 \exp(-U_{eff}/kT) \quad (1)$$

ation rate (τ is the relaxation time), $1/\tau_0$ is the pre-exponential factor, U_{eff} is the effective relaxation barrier, and k is the Boltzmann constant. The fit of the data to Equation (1) gave $U_{eff}=50.1$ K and $1/\tau_0=3.61\times10^8$ s^{-1}. This U_{eff} value is smaller than that of normal $[Mn_{12}]$ complexes; complex **1**, for example, has a U_{eff} of 60–65 K.

The observation of out-of-phase AC signals suggests that **2** might be an SMM, although such signals by themselves are not proof of an SMM. It is also tempting to assume that the two χ_m'' signals in Figure 3 are due to the two crystal forms, diamondlike **2a** and needlelike **2b**. To confirm whether **2a** and/or **2b** are indeed SMMs, and to assess any difference between the two forms, magnetization versus DC field sweep studies were performed on single crystals of **2a** and **2b** by using a micro-SQUID apparatus.[17] The resulting hysteresis loops are shown in Figure 4, and their coercivities 1) increase with decreasing T at a constant field sweep rate, and 2) increase with increasing sweep rate at a constant T (not shown). This situation is as expected for the superparamagnet-like properties of an SMM.

However, it is clear that the observed properties (hysteresis loops) of **2a** and **2b** are very similar, and this is totally

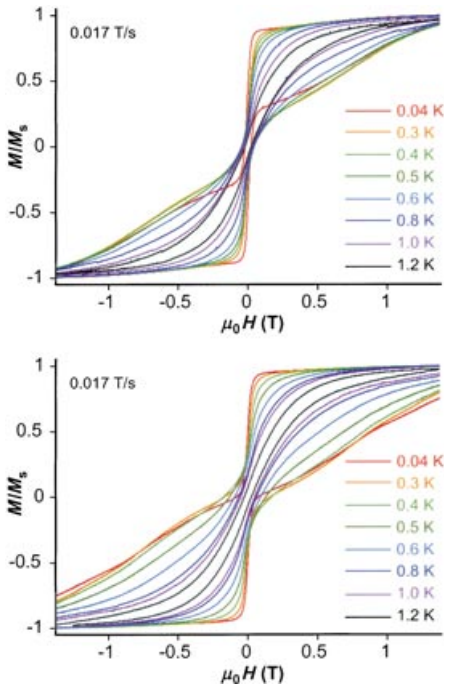

Figure 4. Magnetization (M) versus applied magnetic field ($\mu_0 H$) hysteresis loops for a single crystal (wet with mother liquor) of **2a** (top) and **2b** (bottom) at the indicated temperatures. M is normalized to its saturation value, M_s.

inconsistent with the two very different AC signals in Figure 3 and the at-first-glance "obvious" conclusion that the two signals are due to the two crystal forms. In fact, the hysteresis loops of both **2a** and **2b** suggest a mixture of faster relaxing (LT) and slower relaxing (HT) forms, the faster relaxing being responsible for the large decrease in magnetization at zero field, and the slower relaxing being responsible for the subsequent feature at higher fields. The relative proportions of these two features suggest comparable amounts of the LT and HT forms in each crystal, with perhaps a slightly greater amount of the LT, and this situation is again consistent with the relative proportion of LT and HT AC signals shown in Figure 3. Note that the hysteresis studies were performed on wet single-crystals and the AC studies on microcrystals suspended in solid eicosane, and thus not strictly speaking on the same material. Nevertheless, we conclude that 1) complex **2** is a new SMM, 2) the different space groups of diamond-like **2a** and needle-like **2b** lead to only small differences in the magnetic properties of the $[Mn_{12}O_{12}(O\text{-}Me)_2(O_2CPh)_{16}(H_2O)_2]^{2-}$ ion, and 3) there are faster and slower relaxing forms of complex **2** that cocrystallize in the same crystal. In fact, the existence of cocrystallized faster and slower relaxing forms of **1** has long been known, with crystals of **1** containing about 5% of the faster relaxing form;[6f] in this respect complex **2** only differs from **1** in the relative amounts of the two forms.

For normal $[Mn_{12}]$ complexes, we have reported elsewhere that crystals of pure faster relaxing forms can be prepared with, for example, *tert*-butylacetate as the carboxylate group.[6d,g] Crystallography on such crystals has allowed the origin of the faster relaxing form to be identified as the abnormal orientation of one of the Mn^{III} JT elongation axes, being disposed equatorial rather than axial to the Mn_{12} disk-like plane, and thus this JT axis points towards a core O^{2-} ion. We have named this "Jahn–Teller isomerism". The same effect is likely to be the origin of the two forms of **2**. Indeed, this phenomenon rationalizes the unusual Mn–O bond lengths at Mn4 for **2a** and Mn1 for **2b**. For **2a**, for example, an approximately equal mixture of a) slower relaxing species with the JT axis at Mn4 in the normal position along the O9-Mn4-O14 axis, and b) faster relaxing species with the JT axis at Mn4 abnormally aligned along the O7-Mn4-O12 axis, will lead to the crystallographic average result that the O9-Mn4-O14 bonds are shorter and the O7-Mn4-O12 bonds are longer than they should be, which is what is seen (similarly for **2b**). We thus feel that the crystallographic data support the conclusion from the magnetic studies that crystals of **2a** and **2b** comprise a mixture of slower and faster relaxing species which result from normal and abnormal orientations, respectively, of a Mn^{III} JT elongation axis. As with normal $[Mn_{12}]$ complexes, it will require crystallization of pure crystals of the different forms of **2** to allow more detailed study.

In summary, we have developed access to a variant of the $[Mn_{12}]$ family of SMMs by using a reductive-aggregation route. This structurally very similar variant is also an SMM and, like normal $[Mn_{12}]$ complexes, displays both faster and slower relaxing magnetization dynamics that we assign to the presence of Jahn–Teller isomerism. We have in the past obtained many derivatives of $[Mn_{12}]$ complexes, for example, by carboxylate substitution,[6,7] one- and two-electron reduction,[6f,9,10] introduction of non-carboxylate ligands,[8] and similar derivatization of **2** may also prove possible, in which case it is merely the prototype of what could become a large new family of related SMMs.

Experimental Section

2: Freshly-prepared $(NnBu_4)MnO_4$ (1.0 g, 2.8 mmol) was added in small portions to a solution of benzoic acid (5.0 g, 40.9 mmol) in MeOH (15 ml), and the mixture stirred for about 5 min. The resulting purple solution was left undisturbed at room temperature overnight. During this time, the color slowly turned dark brown, and black crystals slowly formed. These crystals, which were found to be poor diffractors of X-rays, were collected by filtration, washed with MeOH (2×10 mL) and dried in vacuo. The material was recrystallized from CH_2Cl_2/hexanes to give a mixture of diamond-shaped crystals of **2a** and needle-shaped crystals of **2b** in an overall yield of 0.12 g (15% based on Mn). These were collected by filtration, washed with hexanes, and dried in vacuo. Both **2a** and **2b** were good diffractors of X-rays, as long as they were kept in contact with the mother liquor to prevent solvent loss. Elemental analysis of dried solid: (%) calcd for $C_{146}H_{166}N_2O_{50}Mn_{12}$ (**2**·2 H_2O): C 51.45, H 4.91, N 0.82; found: C 51.26, H 4.72, N 0.70. Selected IR data (KBr pellet): $\tilde{\nu} = 3430$ (s, br), 3065 (w), 2965 (w), 2925 (w), 2875 (w), 1598 (s), 1560 (s), 1532 (s), 1492 (m), 1448 (m), 1417 (s), 1306 (w), 1177 (m), 1069 (w), 1026 (m), 838 (w), 718 (s), 675 (s), 625 (m, br), 499 (m) cm^{-1}.

Received: August 5, 2004

Keywords: cluster compounds · Jahn–Teller effect · manganese · O ligands · single-molecule magnets

[1] a) R. Sessoli, H.-L. Tsai, A. R. Schake, S. Wang, J. B. Vincent, K. Folting, D. Gatteschi; G. Christou, D. N. Hendrickson, *J. Am. Chem. Soc.* **1993**, *115*, 1804; b) R. Sessoli, D. Gatteschi, A. Caneschi, M. A. Novak, *Nature* **1993**, *365*, 141.

[2] S. M. J. Aubin, M. W. Wemple, D. M. Adams, H.-L. Tsai, G. Christou, D. N. Hendrickson, *J. Am. Chem. Soc.* **1996**, *118*, 7746.

[3] a) G. Christou, D. Gatteschi, D. N. Hendrickson, R. Sessoli, *MRS Bull.* **2000**, *25*, 66; b) D. Gatteschi, R. Sessoli, *Angew. Chem.* **2003**, *115*, 278; *Angew. Chem. Int. Ed.* **2003**, *42*, 268.

[4] a) A. J. Tasiopoulos, W. Wernsdorfer, B. Moulton, M. J. Zaworotko, G. Christou, *J. Am. Chem. Soc.* **2003**, *125*, 15274; b) A. J. Tasiopoulos, A. Vinslava, W. Wernsdorfer, K. A. Abboud, G. Christou, *Angew. Chem.* **2004**, *116*, 2169; *Angew. Chem. Int. Ed.* **2004**, *43*, 2117; c) D. J. Price, S. R. Batten, B. Moubaraki, K. S. Murray, *Chem. Commun.* **2002**, 762; d) S. M. J. Aubin, N. R. Dilley, L. Pardi, J. Krzystek, M. W. Wemple, L.-C. Brunel, M. B. Maple, G. Christou, D. N. Hendrickson, *J. Am. Chem. Soc.* **1998**, *120*, 4991; e) M. Soler, W. Wernsdorfer, K. Folting, M. Pink, G. Christou, *J. Am. Chem. Soc.* **2004**, *126*, 2156; f) E. K. Brechin, M. Soler, G. Christou, M. Helliwell, S. J. Teat, W. Wernsdorfer, *Chem. Commun.* **2003**, 1276.

[5] a) E. K. Brechin, J. Yoo, M. Nakano, J. C. Huffman, D. N. Hendrickson, G. Christou, *Chem. Commun.* **1999**, 783; b) J. Yoo, E. K. Brechin, A. Yamaguchi, M. Nakano, J. C. Huffman, A. L. Maniero, L.-C. Brunel, K. Awaga, H. Ishimoto, G. Christou, D. N. Hendrickson, *Inorg. Chem.* **2000**, *39*, 3615; c) E. K. Brechin, M. Soler, J. Davidson, D. N. Hendrickson, S. Parsons, G. Christou, *Chem. Commun.* **2002**, 2252; d) L. F. Jones, E. K. Brechin, D. Collison, A. Harrison, S. J. Teat, W. Wernsdorfer, *Chem. Commun.* **2002**, 2974; e) M. Moragues-Canovas, M. Helliwell, L. Ricard, E. Riviere, W. Wersdorfer, E. Brechin, T. Mallah, *Eur. J. Inorg. Chem.* **2004**, 2219; f) C. J. Milios, C. P. Raptopoulou, A. Terzis, F. Lloret, R. Vicente, S. P. Perlepes, A. Escuer, *Angew. Chem.* **2004**, *116*, 212; *Angew. Chem. Int. Ed.* **2004**, *43*, 210; g) A. K. Boudalis, B. Donnadieu, V. Nastopoulos, J. M. Clemente-Juan, A. Mari, Y. Sanakis, J.-P. Tuchagues, S. P. Perlepes, *Angew. Chem.* **2004**, *116*, 2316; *Angew. Chem. Int. Ed.* **2004**, *43*, 2266; h) H. Andres, R. Basler, A. J. Blake, C. Cadiou, G. Chaboussant, C. M. Grant, H.-U. Güdel, M. Murrie, S. Parsons, C. Paulsen, F. Semadini, V. Villar, W. Wernsdorfer, R. E. P. Winpenny, *Chem. Eur. J.* **2002**, *8*, 4867.

[6] a) S. M. J. Aubin, Z. Sun, I. A. Guzei, A. L. Rheingold, G. Christou, D. N. Hendrickson, *Chem. Commun.* **1997**, 2239; b) Z. Sun, D. Ruiz, E. Rumberger, C. D. Incarvito, K. Folting, A. L. Rheingold, G. Christou, D. N. Hendrickson, *Inorg. Chem.* **1998**, *37*, 4758; c) D. Ruiz, Z. Sun, B. Albela, K. Folting, J. Ribas, G. Christou, D. N. Hendrickson, *Angew. Chem.* **1998**, *110*, 315; *Angew. Chem. Int. Ed.* **1998**, *37*, 300; d) Z. Sun, D. Ruiz, N. R. Dilley, M. Soler, J. Ribas, K. Folting, M. B. Maple, G. Christou, D. N. Hendrickson, *Chem. Commun.* **1999**, 1973; e) S. M. J. Aubin, Z. Sun, H. J. Eppley, E. M. Rumberger, I. A. Guzei, K. Folting, P. K. Gantzel, A. L. Rheingold, G. Christou, D. N. Hendrickson, *Inorg. Chem.* **2001**, *40*, 2127; f) H. J. Eppley, H.-L. Tsai, N. de Vries, K. Folting, G. Christou, D. N. Hendrickson, *J. Am. Chem. Soc.* **1995**, *117*, 301; g) M. Soler, W. Wernsdorfer, Z. Sun, J. C. Huffman, D. N. Hendrickson, G. Christou, *Chem. Commun.* **2003**, 2672–2673.

[7] M. Soler, P. Artus, K. Folting, J. C. Huffman, D. N. Hendrickson, G. Christou, *Inorg. Chem.* **2001**, *40*, 4902.

[8] P. Artus, C. Boskovic, J. Yoo, W. E. Streib, L.-C. Brunel, D. N. Hendrickson, G. Christou, *Inorg. Chem.* **2001**, *40*, 4199; b) C. Boskovic, M. Pink, J. C. Huffman, D. N. Hendrickson, G. Christou, *J. Am. Chem. Soc.* **2001**, *123*, 9914; c) N. E. Chakov, W. Wernsdorfer, K. A. Abboud, D. N. Hendrickson, G. Christou, *Dalton Trans.* **2003**, 2243.

[9] a) S. M. J. Aubin, Z. Sun, L. Pardi, J. Krzystek, K. Folting, L.-C. Brunel, A. L. Rheingold, G. Christou, D. N. Hendrickson, *Inorg. Chem.* **1999**, *38*, 5329; b) T. Kuroda-Sowa, M. Lam, A. L. Rheingold, C. Frommen, W. M. Reiff, M. Nakano, J. Yoo, A. L. Maniero, L.-C. Brunel, G. Christou, D. N. Hendrickson, *Inorg. Chem.* **2001**, *40*, 6469.

[10] a) M. Soler, S. K. Chandra, D. Ruiz, E. R. Davidson, D. N. Hendrickson, G. Christou, *Chem. Commun.* **2000**, 2417; b) M. Soler, W. Wernsdorfer, K. A. Abboud, J. C. Huffman, E. R. Davidson, D. N. Hendrickson, G. Christou, *J. Am. Chem. Soc.* **2003**, *125*, 3576.

[11] T. Lis, *Acta Crystallogr. Sect. B* **1980**, *36*, 2042.

[12] a) Crystal structure data for **2**·2 H_2O·4 CH_2Cl_2 (**2a**): $C_{150}H_{174}Cl_8Mn_{12}N_2O_{50}$, M_r=3747.90, orthorhombic, *Pbca*, a = 25.476(2), b = 20.933(2), c = 31.206(2) Å, V = 16642(2) Å^3, T = 173 K, Z = 4, ρ_{calcd} = 1.502 g cm^{-3}, 86166 reflections collected, 14638 unique (R_{int} = 0.1115), $R1$ = 0.0642, w$R2$ = 0.1585, using 7705 reflections with $I > 2\sigma(I)$. Crystal structure data for **2**·2 H_2O·CH_2Cl_2 (**2b**): $C_{147}H_{168}Cl_2Mn_{12}N_2O_{50}$, M_r = 3493.09, triclinic, $P\bar{1}$, a = 16.357(1), b = 17.480(2), c = 17.617(2) Å, α = 105.982(2), β = 111.329(2), γ = 108.680(2)°, V = 3982.5(4) Å^3, T = 173 K, Z = 1, ρ_{calcd} = 1.348 g cm^{-3}, 26397 reflections collected, 17568 unique (R_{int} = 0.0489), $R1$ = 0.0696, w$R2$ = 0.1731, using 8580 reflections with $I > 2\sigma(I)$. The dichloromethane molecules of **2a** and the tetrabutylammonium cations of **2b** were disordered and could not be modeled properly, thus program SQUEEZE, a part of the PLATON package[12b] of crystallographic software, was used to calculate the solvent disorder area and remove its contribution to the overall intensity data. CCDC-246482 (**2a**) and CCDC-246483 (**2b**) contain the supplementary crystallographic data for this paper. These data can be obtained free of charge via www.ccdc.cam.ac.uk/conts/retrieving.html (or from the Cambridge Crystallographic Data Centre, 12 Union Road, Cambridge CB21EZ, UK; fax: (+44) 1223-336-033; or deposit@ccdc.cam.ac.uk); b) PLATON: A. L. Spek, *Acta Crystallogr. Sect. A* **1990**, *46*, 1–34.

[13] a) Bond valence sum calculations for Mn^{III} and Mn^{IV} ions of **2a** and **2b** gave oxidation state values of 2.89–3.02 (Mn^{III}) and 4.00–4.18 (Mn^{IV}); W. Liu, H. H. Thorp, *Inorg. Chem.* **1993**, *32*, 4102.

[14] For example, see a) M. J. Manos, A. J. Tasiopoulos, E. J. Tolis, N. Lalioti, J. D. Woolins, A. M. Z. Slawin, M. P. Sigalas, T. A. Kabanos, *Chem. Eur. J.* **2003**, *9*, 695; b) H. Kang, S. Liu, S. N. Shaikh, T. Nicholson, J. Zubieta, *Inorg. Chem.* **1989**, *28*, 920.

[15] P. King, W. Wernsdorfer, K. A. Abboud, G. Christou, *Inorg. Chem.*, in press.

[16] J. T. Brockman, J. C. Huffman, G. Christou, *Angew. Chem. Int. Ed.* **2002**, *41*, 2506.

[17] W. Wernsdorfer, E. Bonet Orozco, K. Hasselbach, A. Benoit, D. Mailly, O. Kubo, H. Nakano, B. Barbara, *Phys. Rev. Lett.* **1997**, *79*, 4014.

